Crop model- and satellite imagery-based recommendation tool for variable rate N fertilizer application for the US Corn system

Zhenong Jin[1,2] · Rishi Prasad[3] · John Shriver[3] ·
Qianlai Zhuang[1,4]

Abstract Precision nitrogen (N) management for corn has gained popularity due to both economic and environmental considerations. There is sufficient evidence demonstrating that N fertilizer efficiency can be improved by implementing sidedress and variable rate fertilization. In this paper, a crop model- and satellite imagery-based decision-support tool for recommending variable rate N fertilization at a high resolution of 5 m × 5 m is introduced. The sub-field management zones were delineated by overlapping the soil survey geographic (SSURGO) soil map units with wide dynamic range vegetation index (WDRVI)-derived relative productivity zones. The calibrated Agricultural Production Systems sIMulator (APSIM) was used to simulate a range of soil N processes, corn growth and N uptake by assimilating real-time weather data from the National Climate Data Center (NCDC). Sidedress N rates were estimated based on the target rate, N loss via leaching and denitrification, plant uptake and leftover N in the soil. The tool was tested on a 66 ha corn field in Illinois, USA for the growing season of 2015. Results showed that N-Prescription was able to give reasonable management zone delineation and sidedress N recommendation. The recommended sidedress N ranged from 60 to over 120 kg ha^{-1}. Corn yield was greater in areas with higher sidedress recommendation, but the benefit from sidedress decreased with the increasing rate and plateaued above 110 kg ha^{-1}. Sensitivity analysis suggested that soil hydraulic properties and soil organic matter content were

✉ Qianlai Zhuang
  qzhuang@purdue.edu

1   Department of Earth, Atmospheric and Planetary Science, Purdue University, CIVIL 550 Stadium Mall Drive, West Lafayette, IN 47907-2051, USA

2   Department of Earth System Science and Center on Food Security and the Environment, Stanford University, Stanford, CA 94305, USA

3   Farmlogs, Ann Arbor, MI 48104, USA

4   Department of Agronomy, Purdue University, West Lafayette, IN 47907, USA

critical to the sidedress accounting. Corn growth, and hence the cumulative N uptake, can be well simulated by calibrating the WDRVI derived leaf area index. This tool could serve as a good foundation for further development in precision N management.

Introduction

Nitrogen (N) is one of the primary limiting factors for corn (*Zea mays* L.) yield and quality (Scharf 2015). Corn with deficient N will have dwarfed seedlings and yellowish leaves, leading to partial or complete failure of kernel setting (Ma and Biswas 2015). While adequate N is necessary for proper plant development and optimal grain yield, over-fertilizing risks contamination of water at local and regional scales (Keeney and Olson 1986; McIsaac et al. 2002), and nitrous oxide (a potent greenhouse gas) emissions (Park et al. 2012; Scharf 2015). The need to wisely manage N fertilizer is thus compelling for both economic and environmental considerations (Scharf 2015).

In practice, the producer-level associated cost of under-fertilization relative to over-fertilization drives farmers to apply N at greater rates, as additional "insurance" against yield losses (Moebius-Clune et al. 2013). It is estimated that 75% of N fertilizer for the US Corn-Belt (typically covering Iowa, Illinois, Indiana, southern Michigan, western Ohio, eastern Nebraska, eastern Kansas, southern Minnesota and parts of Missouri) is applied before planting (Cassman et al. 2002), among which fall application is more widely practiced than spring application. The N fertilizer loss is highly weather dependent, and is greatest in warm and wet winters (Randall et al. 2003; Tremblay et al. 2012; Scharf 2015). Thus, to reduce N losses before the growing season begins, a good strategy is to apply a portion of N in-season (Thompson et al. 2015). Furthermore, applying N based on soil heterogeneity can reduce the overall N rate applied and increase profitability compared with a uniform N application (Mamo et al. 2003).

The optimal management of N requires a farmer to make a series of decisions on the form (what), timing (when), placement (where) and rate (how much) of N fertilizer to be applied. While the N form and timing is often limited by accessibility and logistic con-straints, determining where and how much N fertilizer should be applied is more science-oriented (Scharf 2015), and has progressed considerably in recent years (Setiyono et al. 2011; Shahandeh et al. 2011; Solie et al. 2012; Moebius-Clune et al. 2013; Thompson et al. 2015). It is well established that the optimal N rate for a given field depends on crop demands, indigenous N supply as a net result of mineralization and immobilization, and losses of N fertilizer or soil-derived N via leaching, denitrification and volatilization. Each of these aforementioned processes interacts among themselves, and is influenced by many factors such as seasonal temperature, precipitation, soil physical and biogeochemical properties, and management history. Although researchers have spent considerable efforts to understand the complexity associated with N management, the uncertainty is still substantial (Scharf 2015). The problem is further complicated by spatial variations in soil N contribution, fertilizer losses and crop N uptake from field to field and even place to place within a field. N mineralization of SOM may vary because of differences in organic N release rate as a function of soil temperature and moisture, or differences in past crop removal (Scharf 2015). N leaching loss can vary mainly because of different topography and soil hydrological properties (Prasad et al. 2015). The N fertilizer needed by the crop

can vary as a result of varying yield potential (Mamo et al. 2003), or differences in seeding rates. Because of these complexities, a fast and accurate diagnostic tool for the optimal N rate for a given field remains a challenge (Ma and Biswas 2015; Scharf 2015).

Crop models that simulate all the aforementioned N processes have been identified as a management tool for synchronizing N fertilizer application with crop N demand (Cassman et al. 2002; Scharf 2015). A number of specific simulation models have been developed to optimize pre-plant or in-season N management from either public research institutes or private sectors, among which Adapt-N (Melkonian et al. 2008; Moebius-Clune et al. 2013; Sela et al. 2016) and Maize-N (Setiyono et al. 2011; Thompson et al. 2015) are two such examples that are still in active development. The Maize-N tool is built on the Hybrid-Maize model (Yang et al. 2006), and estimates the N sidedress based on a spherical function that relates yield to N rate (Setiyono et al. 2011). Maize-N in general recommends substantially more N than sensor-based, in-season N recommendations, but was better at protecting yield (Thompson et al. 2015). The Adapt-N model is built on the Precision Nitrogen Management model (Melkonian et al. 2008), which consists of two major components: (i) a corn growth model adapted from Sinclair and Muchow (1995), and (ii) a biogeochemistry model that simulates water and solute transport (Sela et al. 2016), as well as biochemical transformation of N. Adapt-N calculates N recommendation based on a mass balance approach according to a number of factors, including the required N to achieve the expected yield, N content in crop and soil, N credit from soybean rotation, and a probabilistic estimation of future N gains minus losses (Sela et al. 2016). However, neither Adapt-N nor Maize-N has been tested in terms of their capability to give variable rate N within a field. Also, their operational use often requires the user to input a range of field measurement data, lowering the potential of farmer use at scale.

The recent advent of high-performance computers and communication technologies has made it possible to process massive remotely-sensed or field survey data and weather data in near real-time to inform precision N management. Here for the first time, this study investigates the potential of very-high-resolution (5 m × 5 m) on-farm N management by integrating recent advances in a range of research areas, including remote sensing, crop modeling and soil mapping. The proposed tool uses remotely-sensed data to delineate within-field management zones, simulates sub-field variations in soil and crop status with a crop model that assimilates in situ soil database and real-time weather information, and finally delivers either pre-plant or in-season variable rate N recommendations to match fertilizer application with crop demand. The core part of a process-based crop model for estimating indigenous N supply, N losses and crop N demand is built on the Agricultural Production Systems sIMulator (APSIM) platform (Holzworth et al. 2014). In the following sections, detailed science and engineering background of the N recommendation tool will be described, and a case study for a typical US Midwest Corn field in Illinois, USA, will be presented. The goal of this paper is to introduce a prototype and discuss possible improvements, with a hope that this study will inspire others to investigate further on precision N management.

Materials and methods

Overview of workflow

The N-Prescription infrastructure is built on the Amazon Elastic Compute Cloud (EC2; https://aws.amazon.com/ec2/), and has been parallelized to support multiple simulations at

the same time. Amazon EC2 is a web service that provides resizable compute capacity in the cloud. It is designed to make web-scale cloud computing easier for developers/programmers. The scientific workflow is given in Fig. 1, and major steps include:

(1)   Determine the total and pre-plant N application rate. The total N target rate (N_{target}; kg ha^{-1}) for a given growing season is based on the expected yield goal, N credits and field productivity variations:

$$N_{target} = c_0 + c_1 \cdot (\overline{Y} + \varepsilon) - N_{credit} \qquad (1)$$

where $\overline{Y}$ is the field average yield or attainable yield (t ha^{-1}) derived using the farmer's reported value or by looking at the county-level yield as reported by USDA
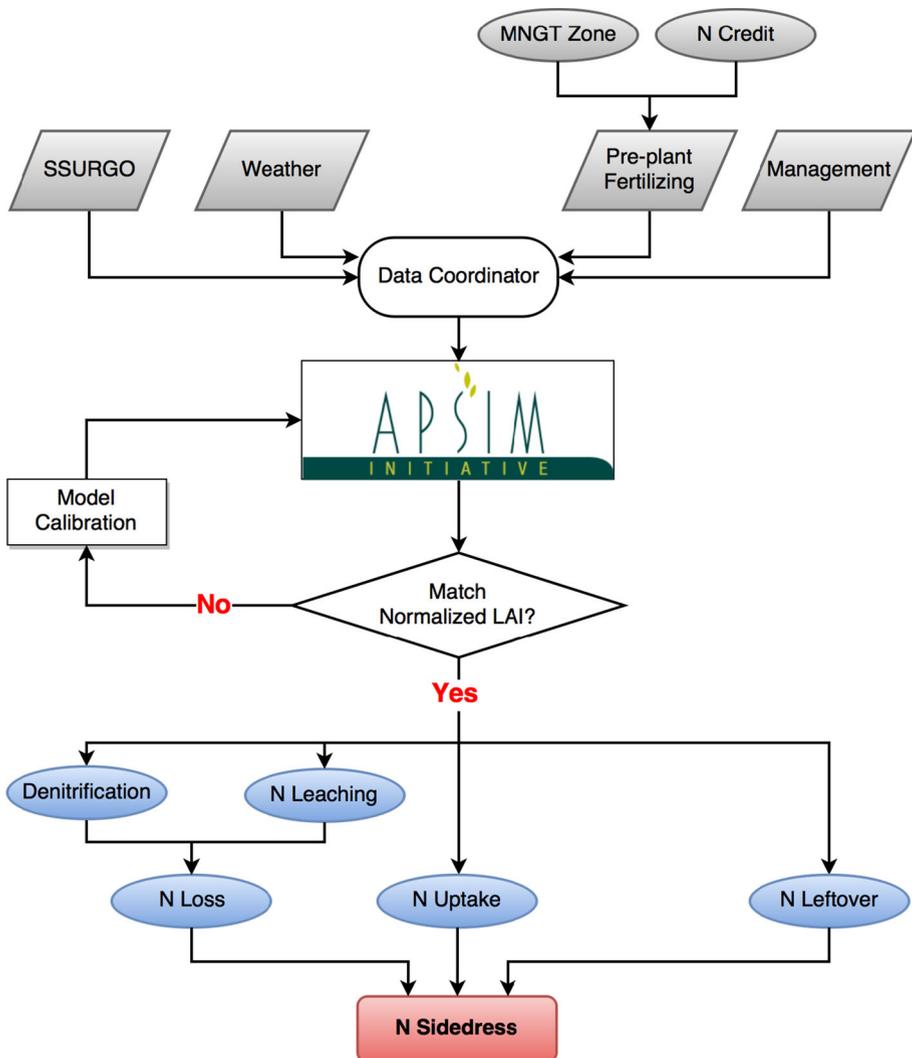
Fig. 1 A schematic diagram for the workflow used in this study to generate the in-season N sidedress

National Agricultural Statistics Service (NASS); ε is the adjustment term that accounts for spatial variability of long-term average soil fertility among productivity zones and can be estimated by looking into the historical yield map generated by harvest combine or derived from the multi-year averaged remote sensing images (see section "The estimation of ε and expected yield" for detailed discussion); $\overline{Y} + \varepsilon$ is thus the expected yield from each productivity zone; c_0 and c_1 is the offset and slope for calculating state-specific N fertilizer requirement per unit yield (Table S1), respectively; N_{credit} is the credits for soil organic N from previous legume crops or manure application (Table S2). Among the N_{target}, 50% is assumed to be applied before planting as either fall or spring application.

(2) Data query. This step essentially collects all data required and creates simulation files for the APSIM. It starts with importing a 5 m × 5 m raster, clipped to the field boundary. Based on the raster extent, soil parameters such as layered soil hydraulic properties, soil pH and soil organic matter (SOM) are queried from the Soil Survey Geographic (SSURGO) database (Soil Survey Staff 2015) and resampled to finer vertical layers with depth 0–0.1, 0.1–0.2, 0.2–0.5, 0.5–1.0 and 1.0–2.0 m. When there are multiple soil components within a grid, the largest fraction will be selected. Detailed descriptions for soil parameters required for the model are presented in Archontoulis et al. (2014). These parameters can be further refined once onsite soil sampling data is available. Real time weather data for the site, including daily maximum and minimum temperature, precipitation and solar radiation are from the National Climate Data Center (NCDC), Asheville, NC, USA. Field management information including sowing date, seeding rate and cultivar relative maturity is input by users if available; otherwise, estimated values according to satellite imagery and NASS report are assigned.

(3) Crop model simulation. The APSIM is run at a daily time step to provide soil and crop N status, such as N leaching and denitrification, N leftover in soil and plant N uptake. Instead of running the model for the whole field, the tool run the model for virtual grids first, and then re-project outputs to the 5 m-resolution raster shapefile according to a geographic reference table. A virtual grid is a unique combination of soil type, seeding rates and management zone. For example, if there are 5 different soil types, four levels of seeding rates and five productivity zones for a given field, the number of virtual grids is 100. Using virtual grids substantially lowers the computational cost. When observational data such as satellite or UAV imagery is available, the crop model will be calibrated iteratively to match spectral-derived vegetation indices (e.g. LAI).

(4) Calculating sidedress N rate. The sidedress N fertilizer rate ($N_{sidedress}$) is computed using the equation:

$$N_{sidedress} = N_{target} + N_{loss} - N_{uptake} - N_{leftover} \tag{2}$$

where N_{loss} is the total N losses via denitrification (N_{denit}) and leaching (N_{leach}) up-to-date, N_{uptake} is the cumulative plant N uptake when sidedress N recommendation is requested, and $N_{leftover}$ is the remaining inorganic N up-to-date. The timing of sidedress N application is assumed to be around V6 stage (Abendroth 2011), after which rapid crop N uptake will happen. The N loss after sidedress is not explicitly accounted for in the current framework, since both denitrification and leaching during the remaining growing season are highly weather dependent and difficult to

forecast. The N loss after sidedress application is assumed to be partly compensated by gains of N via net mineralization of soil organic matter.

Management zone delineation

Management zone refers to the relatively homogeneous sub-units of a field, within which a uniform management practice can be applied (Mulla 2013). Several approaches have been developed to delineate site-specific management zones, such as based on soil characteristics (Fleming et al. 2004), yield maps from multiple years (Diker et al. 2004), remotely sensed spectral information (Zhang et al. 2010; Cicore et al. 2016), or more often based on a combination of multiple data (Song et al. 2009; Shaddad et al. 2016). These layers of information can be processed by various clustering algorithms to generate the management zones, among which Fuzzy-k mean is so far the most popular option (Guastaferro et al. 2010). In this study, the management zones are delineated by combining the satellite observed multi-year crop productivity and the soil types derived from SSURGO.

For a given field, the delineation starts with identifying the sub-field relative productivity zones based on the wide dynamic range vegetation index (WDRVI) derived from RapidEye images. The RapidEye system is a constellation of five satellites that produces multispectral images at a spatial resolution of 5 m × 5 m; detailed description of radiometric and geometric properties of the RapidEye sensor is given in Chander et al. (2013). The red (630–685 nm) and near infrared red (NIR) (760–850 nm) bands are used to calculate the WDRVI following Gitelson (2004):

$$WDRVI = \frac{\alpha \rho_{NIR} - \rho_{red}}{\alpha \rho_{NIR} + \rho_{red}} \tag{3}$$

where ρ is the reflectance and α is a weighting coefficient set to be 0.2. Main steps to classify the relative productivity zones include:

(1) Collect all WDRVI images between July 15th and September 1st for years 2009–2014 that are at least 90% cloud free. The time window from middle July to early September is selected because previous studies showed that remotely sensed vegetation indices during this period are most indicative for the final corn yield (Sibley et al. 2014; Lobell et al. 2015). The Landsat-7 cloud filtering algorithm (Irish, 2000) for automatic cloud cover assessment is applied to the radiometric data in the Rapideye dataset, adjusting the thresholds based on a training dataset collected over 50 images in the Midwestern US between 2009 and 2014.

(2) Apply L1 normalization to the WDRVI data (i.e. for each image, subtract the minimum and then divide by the maximum). Pixels within 15 m of the field edge were excluded, as field edges tend to show lower yields and WDRVI, but are too narrow and costly to manage as separate zones.

(3) Average all the images within a year to generate a single image per year.

(4) Pass all the normalized annual mean images (one per year when data are available) to an unsupervised k-means algorithm (Arthur and Vassilvitskii 2007) for classification. The k-means algorithm, implemented in the "scikit-learn" package for Python, divides the image pixels (x) into k clusters, by iteratively optimizing the choice of cluster specific centroids (c) that can minimize the total within-cluster distance between individual pixels and the corresponding centroid:

$$D_{total} = \sum_{j=1}^{k} \sum_{i=1}^{n_j} ||x_i^{(j)} - c_j|| \tag{4}$$

where $x_i^{(j)}$ is the ith pixel in jth cluster, and n_j is the number of pixels classified into the jth cluster. The gap statistic (Tibshirani et al. 2001) is used to estimate the number of clusters (i.e. k) present in the dataset. The resulting clusters are labeled as different productivity zones. These productivity zones will then be overlaid with the SSURGO map units, and each unique combination of productivity zone and soil map unit is treated as a separate management zone (Fig. S1).

Description of the APSIM

The APSIM is an agricultural system model that can simulate the growth of a number of crops under various climatic, edaphic and management conditions (Holzworth et al. 2014). In this study, the maize module in APSIM version 7.7 was used to model the phenology, morphology, and biomass production for corn. The phenological phase progress was simulated using the thermal time method (Wilson et al. 1995), and the radiation use efficiency (RUE) based biomass production and partition was limited by temperature, water and N stress (Hammer et al. 2009). The APSIM has recently been widely applied in the US Corn-Belt to address a range of research questions related to the corn production and cropping system management (Hammer et al. 2009; Lobell et al. 2013; Archontoulis et al. 2014; Jin et al. 2016).

The SoilN module simulates the dynamics of soil carbon (C) and N on a daily basis, with N mineralization, immobilization, nitrification, denitrification and urea hydrolysis explicitly described in each soil layer. The layer-specific SOM is divided into a fast decomposing pool (BIOM) and a less active pool (HUM). To account for the age of different organic residuals, part of the HUM pool is further specified as a recalcitrant pool (INERT), with the fraction to be larger in deeper soil layers. Organic N sequestrated by SOM will be gradually released through mineralization according to the decomposing of each soil C pools, with the rate mediated by soil temperature, moisture and C/N ratio. More fresh organic matter is stored in a separate pool (FOM), and is initialized by root weight and root C/N ratio. The FOM pool contains three sub-pools, namely the carbohydrate-like, cellulose-like and lignin-like pools, with default fractions set as 0.2, 0.7 and 0.1, respectively. The APSIM also supports manure application through the SurfaceOM module, which describes the organic N fractions in the same way as the FOM pool. When N fertilizer is applied, the N will enter the inorganic N pools of Urea-N, NH_4-N and NO_3-N, with the fraction determined by the fertilizer type.

These soil N processes are primarily controlled by soil temperature, moisture, pH and water flow through the soil profile. Daily soil temperature for each soil layer is simulated by the SoilTemp module. Soil hydrology is simulated by the SoilWat module that uses a cascading water balance model approach (Littleboy et al. 1992). This daily time-step hydrology model includes: surface runoff (estimated via the USDA curve number method), soil evaporation (estimated via the two-stage evaporation method), plant transpiration (estimated via the transpiration efficiency approach), and vertical water flows and fluxes that can transport N in soil solute through the soil profile. Parameters for these soil modules are mainly derived from the SSURGO database, and a few are obtained through calibration.

SSURGO database

The SSURGO database is a compilation of county soil surveys by the USDA Natural Resources Conservation Service (NRCS), and is typically available for most of the US territories at a scale of 1:24 000. The SSURGO uses georeferenced map units to depict the spatial distribution of soil components. Within each map unit, the fraction of the component soils and their layer-specific properties are explicitly given. In this study, soil information from SSURGO is queried using the R soilDB package that can interact with the NRCS soil data access (SDA) web service. More details about the implementation of soilDB are available at: http://ncss-tech.github.io/AQP/soilDB/SDA-tutorial.html (last accessed 31 October 2016).

Although the only available option for widespread soil information in the focus region of this paper, SSURGO has been questioned for not accurately representing the actual field variability (Ashtekar and Owens 2013). In application, part of the required soil parameters, such as soil texture and soil organic matter content, may be further tuned when onsite soil sampling is available. Yet in the APSIM, the simulation of soil N and hydrological processes are controlled by more than one hundred parameters. What are the most important parameters to measure remains an open question. As a starting point, a global sensitivity analysis (GSA) was conducted following Pappas et al. (2013) to identify the most sensitive soil parameters for N uptake, denitrification, leaching and net N mineralization. Detailed implementations of the GSA are presented in the Supplementary Material (Text S1), and candidate parameters along with their initial values are listed in Table S3.

Model calibration

Traditional model calibration for a specific location requires a range of field measurement and is very labor-intensive (Archontoulis et al. 2014), and thus is not suitable for developing a computationally efficient and spatially extensible N management tool. In this prototype, model calibration mainly focuses on matching the early season LAI. In the APSIM, LAI directly controls the canopy intercepted solar radiation, which limits the biomass production, and the accumulated biomass will in turn be allocated to build LAI. Because of this feedback, any bias in LAI simulation (especially in early seasons between emergence and V5/V6 stages) will lead to unreasonable simulation of corn growth and N uptake. On the other hand, APSIM by default tends to substantially underestimate the early season LAI, and hence crop N uptake. Therefore, the current calibration was primarily for correcting the systematic underestimation of LAI in the early season.

Ideally this should be done by calibrating the APSIM LAI simulation against a series of observed spectral information of the current growing season up to the date when N sidedressing is calculated. However, cloud-free satellite images are often too limited for the period between crop emergence and V5/V6 stages to give sufficient degrees of freedom for observations. One feasible solution is to use UAV images that can be obtained with higher temporal frequency, which is out of the scope of this study (the pros and cons of this solution will be discussed later). Alternatively, when high quality WDRVI images are sufficient for the previous year, it is feasible to derive parameters by calibrating the model using WDRVI values of the previous year. The two underpinning assumptions are: (i) the cultivar grown in the same field is similar between two years, and (ii) calibration for the whole season LAI curve helps to reduce the underestimation in early season. Here, two methods for LAI calibration were introduced. The first method (named Calibration-1

hereafter) was to match the absolute LAI curve by adjusting four key parameters, namely, *breadth* (determines the width of LAI seasonal curve), *skewness* (determines the LAI change rate), *area_max* (determines the max potential LAI), *largest_leaf* (determines when the max potential LAI occurs). This method was used to generate a sidedressing prescription in a case study described below. The second method (named Calibration-2) was developed more recently, which uses a cost function based on the normalized LAI curve. The phenology parameters adjusted in Calibration-2 method are *leaf_init_rate* (degree days to initiate each leaf primordium until floral initial), *leaf_app_rate1* and *leaf_app_rate2* (growing degree day required to develop the leaf ligules of two stages), and *leaf_no_dead_slope* (coefficients for rate of leaf number senescence after flowering). The sensitivity of parameters in both Calibration-1 and Calibration-2 on LAI is shown in Fig. S2. The shuffled complex evolution Metropolis algorithm (SCEM-UA), an adaptive Markov Chain Monte Carlo (MCMC) sampler, was implemented to globally optimize these parameters (Jin et al. 2015).

The WDRVI to LAI conversion was based on the empirical relationship built by Viña et al. (2011) in the form of:

$$LAI = \frac{1}{b}[ln(a) - ln(a + y_0 - WDRVI)] \qquad (5)$$

where $a = 1.4392$, $b = 0.3418$ and $y_0 = -0.6684$. One concern about estimating LAI using Eq. 5 is that such a relationship is derived from a limited number of sites and may not have generality. The uncertainty associated with applying Eq. 5 can be substantially reduced when using the Calibration-2 method. To support this argument, a comparison is presented for the estimated LAI and normalized LAI using artificial variants of Eq. 5 by sampling the coefficients a, b and y_0 within a range of $\pm15\%$.

Case study

To test the robustness of this prototype, the tool was applied to a representative US Midwestern rainfed corn field ($40.4°N$, $-88.2°W$) in Illinois (Fig. 2. For the 2015 growing season, the farmer applied 112 kg ha^{-1} spring fertilizer in forms of Urea N on Mar 24th; seeds were sown at variable seeding rates with 0.75 m rows on May 25th (Fig. 3a); a mixture of three corn varieties with the same relative maturity ratings were planted. The cultivar-specific parameters were adopted from a similar cultivar for the US Corn-Belt, the Pioneer_P04612XR_106 (see Table 4 in Archontoulis et al. 2014). The prescription for sidedress N was requested on June 24th, and applied by a variable rate fertilizer applicator during the following week. The corn was harvested on October 18th. The coefficient used to calculate N_{target} using Eq. 1 was: 0 for c_0, 1.2 for c_1, 202 kg ha^{-1} for $\overline{Y}$, and -20, -10, 0, 10 and 30 kg ha^{-1} (approximately -10, -5, $+0$, $+5$, $+15\%$ of the median level) for ε ranging from the low to high productivity zone; N_{credit} is 0 for this continuous corn field. The values for ε are estimated based on the multi-year averaged yield for each productivity zone derived from the combine yield map, except the very high level of $+15\%$ is arbitrarily designed (which should be $+10\%$ according to the yield map) for sensitivity test purposes.
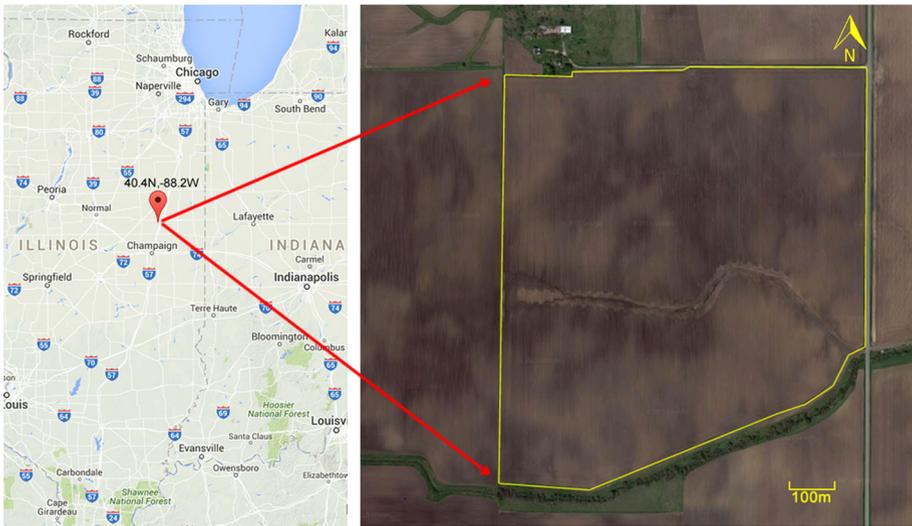
Fig. 2 Study area (the focus field is *highlighted* by the *yellow polygon*) (Color figure online)
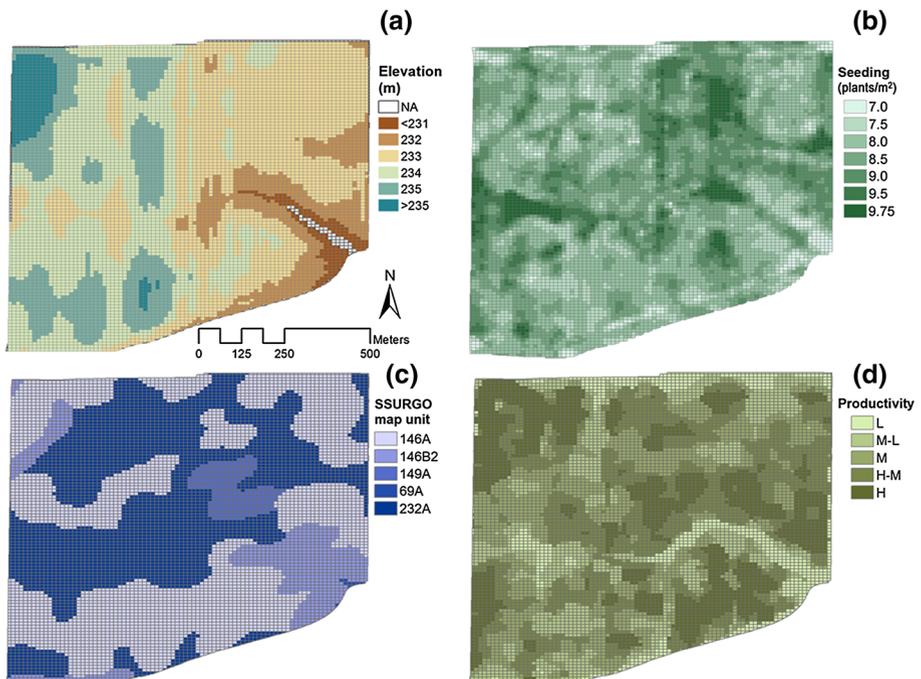
Fig. 3 Spatial delineation of the case study farm based on **a** elevation measured by combine GPS, **b** seeding rates used for the 2015 growing season, **c** soil map units from SSURGO database ("146A" denotes Elliot silt loam soil, "146B2" denotes Elliot silty clay loam soil, "149A" denotes Brenton silt loam soil, "69A" denotes Milford silty clay loam soil and "232A" denotes Ashkum silty clay loam soil), and **d** relative productivity derived from multi-year averaged WDRVI data, ranging from low (L), low–median (L–M), median (M), median–high (M–H) to high (H)

Results and discussion

Management zone delineation

The delineation of relative productivity zones derived from the 5-year averaged summer time WDRVI is shown in Fig. 3d. High productivity zones accounted for 24.3% of the whole field, and were found mainly in the northwest and southeast parts of the field. Low productivity zones accounted for 9.6%, and distributed as a striped channel stretching from the southeast to the middle of the field. Such a channel was also identified from the Google Earth bare soil imagery (Fig. 2). High–median, median and median–low productivity zones accounted for 26.7, 23.1 and 16.3%, respectively. Sub-field variability of productivity zones was comparable to bare soil colors, with high productivity zones generally occurring in light colored soils and low productivity zones corresponding to dark soils (Figs. 2, 3d). Such a spatial pattern contrasted the prevalent expectation that darker soils with more SOM in general had higher fertility (e.g. Ladoni et al. 2010; Scharf 2015). One possible explanation is that dark-colored soils were prone to flooding as they had on average lower elevation than surrounding areas (Fig. 3a), thus receiving little benefit from greater humus accumulation. It is also likely that the spectral properties of surface soils may not reflect the fertility of deeper soils. These speculations echo Fleming et al. (2004), who found that management zones retrieved from soil colors differed substantially from the results derived from the soil apparent electrical conductivity (EC_a), and the latter approach was more effective in identifying the expected spatial variability in a case study. The configuration of satellite derived productivity zones were not consistent with the SSURGO soil map (Fig. 3c, d), suggesting more efforts are required to transfer soil survey data into directly usable information for sub-field precision management. The final management zones generated by overlaying soil types and productivity zones are presented in Fig. S1.

Management zone delineation was so far a critically uncertain step of this prototype. To date, an efficient and accurate procedure for creating management zones is still lacking, and no single method fits all situations (Derby et al. 2007). This study utilized the satellite imagery of crop growth to delineate the management zones, mainly because of the efficiency and scalability of this approach. Canopy sensor- or grid soil sampling-based approaches for in-season N recommendation may be more reliable as they are based on field measurements, but the considerable labor cost negates the accuracy (Scharf 2015). Soil EC_a is more cost-effective than the traditional fieldwork based approach, whereas its interpretation often requires the use of additional georeferenced data and expert experience. In cases of low yield due to unfavorable weather conditions, the economic benefit from EC_a measurement may not outcompete the costs (Derby et al. 2007). Topography (e.g. elevation) has long been identified as a yield-limiting factor (Kravchenko and Bullock 2000). With the advent of high-quality topographic data, soil survey databasse in conjunction with terrain attributes such as elevation, topographic wetness index, slope percentage and modified catchment area can be used to generate digital maps that better represent the soil functions (Ashtekar and Owens 2013; Chaney et al. 2016). Future research efforts will focus on integrating the geospatial information of soil reflectance and topography into the management zone delineation.

Soil parameter sensitivity and LAI calibration

The qualitative GSA in general identified "cn2_bare" (Runoff curve number for bare soil), "density" (crop population density), "fbiom" (fraction of BIOM pool in SOM), "finert" (fraction of inert pool in SOM), "NO_3"(soil nitrate concentration), "oc" (organic carbon), "SummerCona" (stage I soil evaporation coefficient), "SummerU"(stage II soil evaporation coefficient), "sw"(initial soil water content) and "swcon"(soil water conductivity) (alphabetic order) as the ten most sensitive parameters, although slight variations existed among different model outputs of interest and soil type (results not shown). For quantitative GSA, the total parameter sensitivity based on 20 000 model simulations for each combination of interested model output variable and soil type is summarized in Fig. 4. The most influential parameter for N_{uptake} was "oc", which accounted for nearly 50% of the total variability and was followed by "finert", "fbiom" and "swcon" that each explained more than 10% of the variability. Over 75% of the variability in simulated N_{dnit} can be attributed to the uncertainty of "swcon", much more than the 25% share taken by "oc" (Fig. 4b). "cn2_bare", "NO_3", "oc", "sw" and "swcon" were important parameters to explain the variability in N_{leach} indicating water drainage and N forms were critical processes controlling leaching loss. The uncertainty in *netNmin* can be mainly explained by "fbiom", "finer" and "oc" (Fig. 4d). Differences between soil types were small for all variables investigated except for N_{leach}, which was highly dependent on soil hydraulic properties.
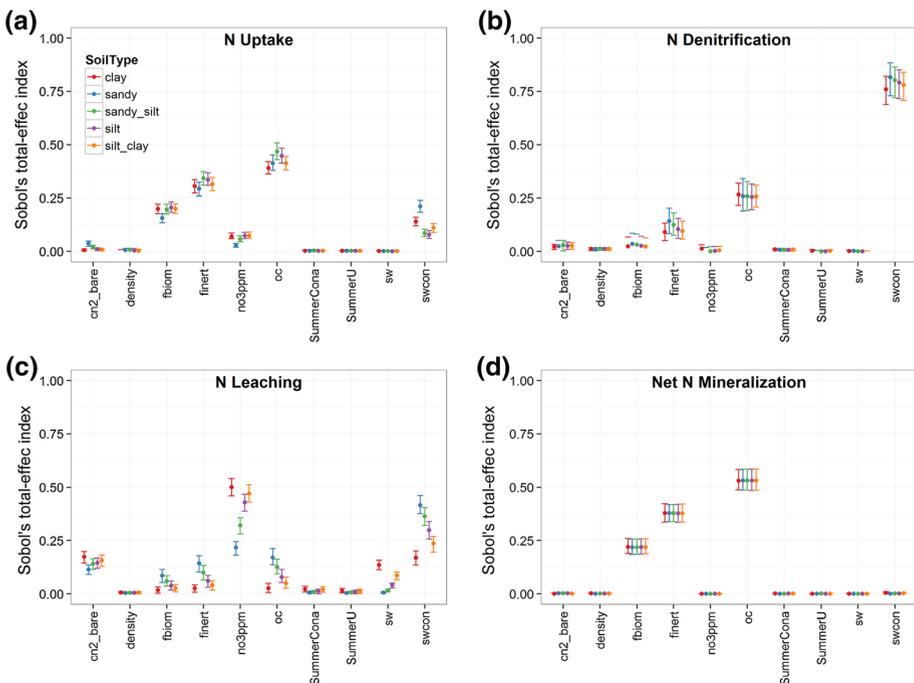
Fig. 4 Sobol's total-effect indices of parameter sensitivity for cumulative **a** plant N uptake, **b** denitrification, **c** N loss through leaching, and **d** net N mineralization under five generic soil conditions (Color figure online)

Sensitivity analysis demonstrated that soil water conductivity and the amount and composition of SOC are the most sensitive parameters to explain the variability in each of the model outputs of interest. Apart from the soil parameters investigated in the GSA, the importance of hydraulic parameters such as saturated water content (SAT in APSIM), water holding capacity (DUL in APSIM) and wilting point (LL15 in APSIM) to all above-mentioned processes are well established as well (Tremblay et al. 2012; Scharf 2015). These hydraulic parameters, along with soil water conductivity, have a robust relationship with soil texture (Saxton and Rawls 2006). Therefore, the uncertainty of the in-season N recommendation can be well constrained if there is better knowledge about the within-field heterogeneity of SOC and soil texture, both of which are more likely to be estimated in a scalable way (Mulder et al. 2011; Castaldi et al. 2016).

By using the SCEM-UA method, *Calibration-1* improved the 2014 LAI simulation, especially for the V5/V6 stage when rapid canopy growth starts in response to a high rate of N uptake (Fig. 5a). The root mean square error (RMSE) decreased from 0.526 m^2 m^{-2} for the simulations with default parameters to 0.258 m^2 m^{-2} for the optimized set. For the 2015 growing season, using the optimized parameters increased the simulated field average LAI on June 22nd from 0.053 to 0.269 (LAI curve not shown), and hence three times more plant N uptake than simulations with default parameters. The normalized LAI based on the Calibration-2 method was slightly more efficient than using the Calibration-1 method in matching the early season LAI given the same number of SCEM-UA runs (Fig. 5a), although they were almost equal in optimizing the RMSE of the whole season LAI observations (0.258 for Calibration-1 vs. 0.259 for Calibration-2). The calibration method showed that assimilating WDRVI data into the APSIM model can reduce the uncertainty in LAI simulation, which further improves the prediction of crop growth and N uptake. Interestingly, estimating LAI by variants of Eq. 5 generated high uncertainties, especially around the period of peak canopy growth (Fig. 5b). Yet normalized LAI was much less affected by the selection of a specific Eq. 5 variant (Fig. 5c). This contrast implied that uncertainties associated with the estimation of LAI from WDRVI images can be effectively reduced by using normalized LAI.

Sub-field sidedress recommendation

By the time that N sidedress was requested, N_{loss} via denitrification and leaching for the farm was considerable (Fig. 6a), accounting for an average of 20% of the spring N application. Sub-field variations were mostly delineated by soil types (Fig. 3b). However, the highest loss mainly came from the Ashkum silty clay loam soil (map unit 232A) with greater SOM, suggesting greater spring mineralization might have led to greater N loss under certain conditions. The variations in N_{uptake} were small, with the majority grids showing N uptake between 20 and 25 kg ha^{-1} N (Fig. 6b), indicating substantial N uptake had not yet happened at this stage. The spatial patterns of N_{uptake} did not follow either soil types or management zones, yet were close to the seeding rates (Fig. 3b). Grids with denser corn population in general showed more N uptake. The sub-field variability of $N_{leftover}$ was primarily characterized by indigenous soil supply potential, while N_{loss} and N_{uptake} played secondary roles (Fig. 6c). The recommended $N_{sidedress}$ rates followed the management zone distribution (Fig. S1), with secondary variability further identified by other factors (Fig. 6d). Very high rates (>120 kg ha^{-1}) accounted for 8.1% of the total field, because these parts had high yield potential. The field average sidedress rate was 92.8 kg ha^{-1}, and was close to the difference between the N_{target} and flat rate of pre-plant application. Thus
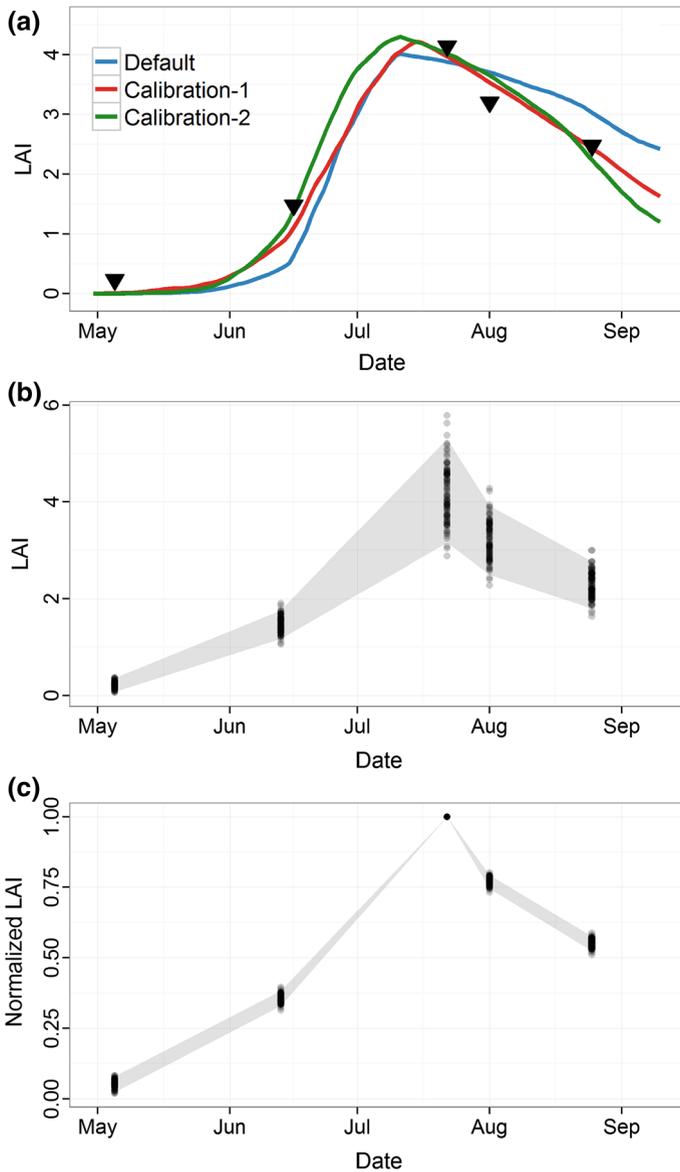
Fig. 5 **a** Model simulated leaf area index (LAI; m² m⁻²) using default (*blue*), calibrated method 1 derived (*red*) and calibration method 2 derived (*green*) parameters. *Black triangle* represents the 90% quantile of field average LAI converted from the WDRVI. **b** Estimated LAI from WDRVI images based on an ensemble of conversion functions. **c** Estimated normalized LAI from WDRVI images based on the same ensemble of conversion functions in (**b**) (Color figure online)

the strategy of variable fertilizing did not necessarily increase the total fertilizer demand, but rather allocated resources from zones with high loss potentials to the ones with high use efficiency. A RapidEye image was acquired on July-14th, 2015, approximately two weeks after the sidedress, and converted to LAI (Fig. 6e). Patches with high LAI values (i.e.
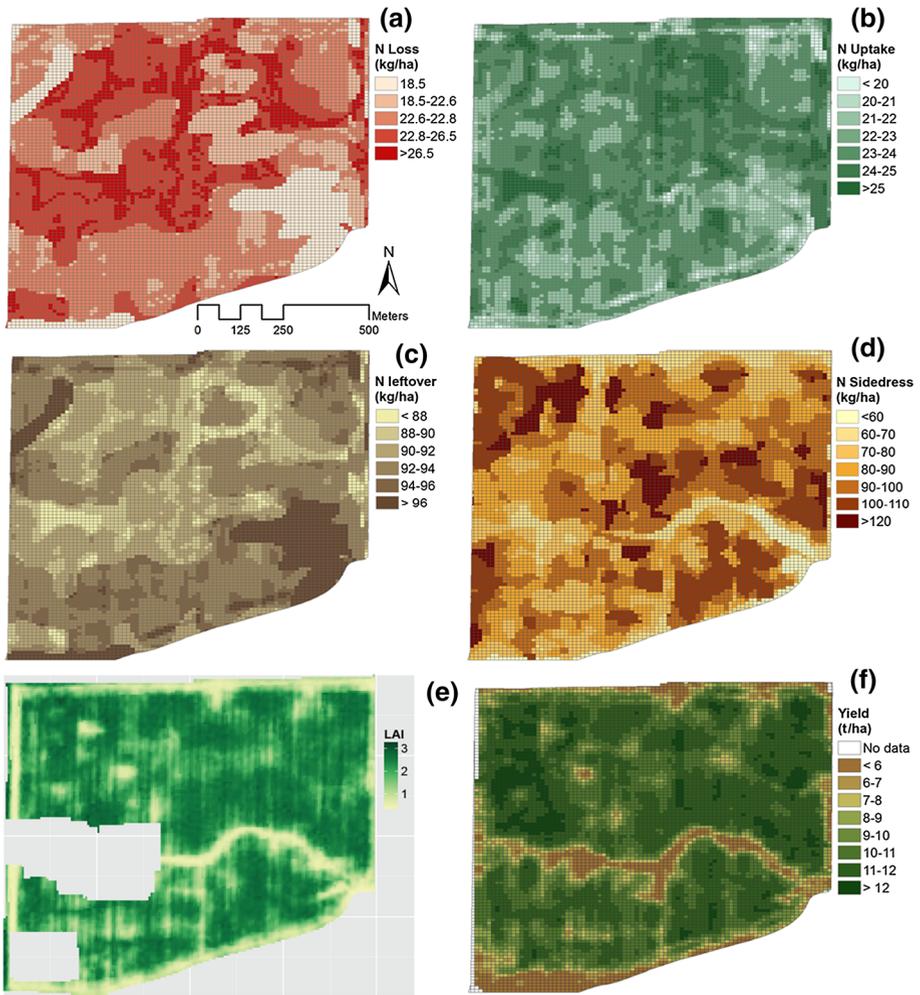
Fig. 6 The spatial variation of model simulated **a** N loss, **b** plant N uptake, **c** N leftover in soil, and **d** N sidedress rate. **e** LAI from RapidEye imagery acquired on July-14, 2015. **f** Harvested yield for 2015

denser corn canopy) closely followed the $N_{sidedress}$, showing that the field crop responded quickly to the sidedress fertilizer. The low LAI strips on the image border were likely due to delay in N discharge when the tractor was operating.

It should be noted that without assigning a spatial adjustment term (ε) in Eq. 1, the recommended N sidedress had much smaller variations (range from 78.4 to 86.6 kg ha^{-1}). The lack of spatial variability was somewhat surprising given the heterogeneity that existed due to combination of soil type, elevation and plant population, but the same was also reported in other studies (e.g. Derby et al. 2007). This was mainly because the N_{loss} was small and N_{uptake} was similar within the field before rapid growth occurred in the V5/V6 stage. Adding an adjustment term thus helped to account for the spatial variation in N denitrification, leaching and differential crop yield potential. After the sidedress, the model

could be run progressively by assimilating new weather data and monitoring the soil and crop N state throughout the remaining growing season to alert N stress occurrences.

The harvested yield for 2015 differed substantially within the field, with low yield patches amounting to less than 6 t ha^{-1} and highest yield up to 12.8 t ha^{-1} (Fig. 6f). The spatial variability in yield was comparable with variable sidedress rates (Fig. 6d), with greater yield occurring in places where greater sidedress N was applied. The low yield strip stretching from southeast to west is also easily identified, matching closely to the low fertilized zone in Fig. 6d. Zonal mean yield based on four different ways of delineating the field is given in Fig. 7. Average yield was close among grids with seeding rates between 7.5 and 9 plants m^{-2}, and was approximately 2.6 t ha^{-1} higher than the average yield from zones with 7 plants m^{-2} (Fig. 7a). However, further increasing the seeding rate above 9.5 plants m^{-2} decreased the average yield, possibly because higher plant population competed for resources. As was expected, average yield increased gradually along the multi-year WDRVI derived productivity zones (Fig. 7b), showing the method proposed to delineate the productivity zone was robust. Yield differences were insignificant among major soil map units (except for map unit 69A which occupied less than 1% of the field area), while standard deviations were large within map units (Fig. 7c). This further confirmed the fact that the heterogeneity of some key soil properties was overlooked by the SSURGO database. Average yield in general increased with the level of sidedress rate, with the marginal benefit more obvious for lower levels (Fig. 7d).
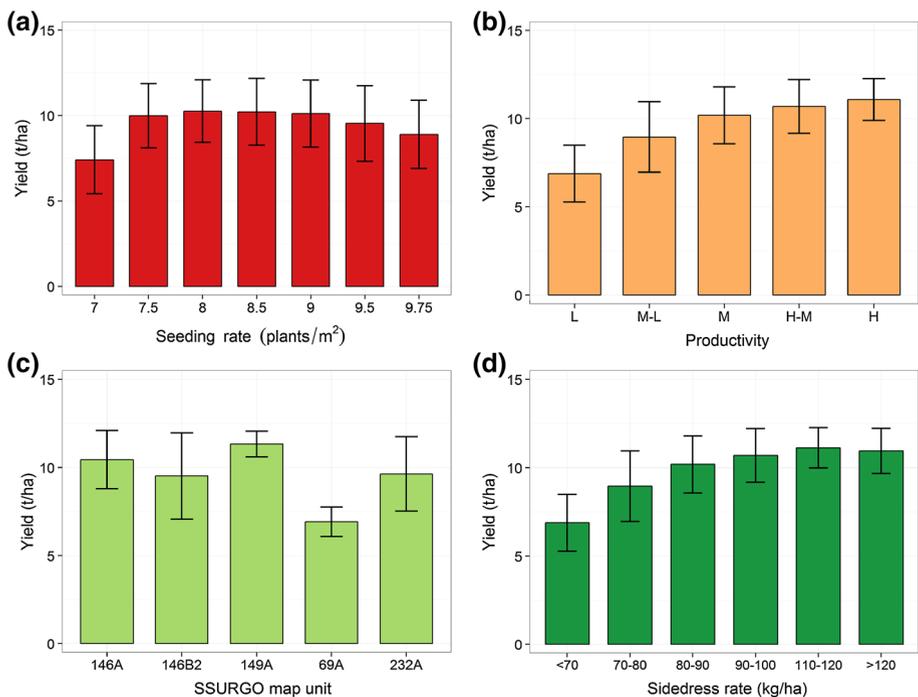
Fig. 7 Zonal statistics for average yield. Zones are delineated according to **a** seeding rate, **b** relative productivity, **c** SSURGO map unit, and **d** N sidedress rate. *Error bars* represent one standard deviation

Uncertainty and potential improvements

The estimation of ε and expected yield

When estimating the target N rate using Eq. 1, user input of $\overline{Y}$ is preferred because growers often know average yield for their field. The more challenging part was to estimate the productivity adjustment term, ε, which is one of the key drivers in creating a wide range of N sidedress rate. In the case study, values for ε were derived from multi-year yield maps, which may not be easily available under most circumstances. The simplest one step forward is to estimate the relative productivity directly based on the averaged multi-year growing season WDRVI values for each productivity zone, since the empirical relationship between corn yield and WDRVI information has proved robust for the US Corn-Belt (e.g. Sakamoto et al. 2014). Moreover, a number of scalable methods that do not require field-based measurements can be potentially implemented to estimate the within-field variation in crop productivity and hence soil fertility. These approaches either relate yield to the absorbed photosynthetically active radiation (APAR) (which can be estimated from satellite data) and light use efficiency (LUE) or regression relationships between remotely sensed vegetation indices and crop yield. A good summary is given in Sibley et al. (2014), among which the approach (named Scalable Crop Yield Mapper, SCYM here after) introduced by Lobell et al. (2015) is most promising since it requires the least number of satellite images and almost no ground-based information and can provide estimates with very high spatial resolution. The SCYM approach uses simulated ensemble of LAI and yield by crop models as pseudo-observations to train a regression that relates final crop yield to satellite observable vegetation indices and a few growing season key meteorological variables. When applying the regression for the field, the current version of SCYM only requires satellite observations for two dates that are not too far away (e.g. 40 days) from the peak growing season. Although not accurate enough for an individual year, the estimation derived from the SCYM approach is much less uncertain for the multi-year averaged yield. These features makes SCYM a promising fit to the current framework that is built on the high spatial resolution RapidEye images that cover multiple years yet are temporally sparse.

Assimilate satellite images to improve model performance

One caveat to be mentioned is that the number of WDRVI images used for LAI calibration is only a little more than the number of parameters to be calibrated, thus lowering the credibility and efficiency of our calibration. The limited number of image acquisitions was mainly because of the bad weather conditions and the budget cap for developing this prototype, but can be potentially solved by increasing the temporal frequency of image request. In fact, the RapidEye constellation allows for daily revisit upon request through off-nadir but low view angle (never exceed 20°) observation, although weekly collection may be sufficient for LAI calibration. This feature is utilized by an updated version (personal communication) of the Agriculture Information Service Platform introduced in Honda et al. (2014). In the coming years, new commercial satellite systems will deliver even better images that can overcome both spatial and temporal scaling challenges in the near future (e.g. the PlanetScope Satellite Constellation). Alternatively, more detailed and frequent canopy information can be obtained through the UAV-based multiple-spectral imaging (Hunt et al. 2008), although it is not yet clear when a UAV system that has the

capability to serve the demand from a large geographic span (e.g. the US Corn-Belt) will become available. Once more spectral information is available, the proposed tool can be easily adapted to do LAI calibration for the current growing season rather than the previous year as presented in the case study. In addition, crop model estimations for both the above ground (e.g. biomass, LAI and crop N uptake) and below ground variables (e.g. soil moisture and hydraulic properties) can be improved by using the existing data assimilation and inverse modeling techniques (Charoenhirunyingyos et al. 2011; Machwitz et al. 2014; Hank et al. 2015).

Soil heterogeneity

As is shown in the sensitivity analysis, soil texture and SOM are vital to the uncertainty of the in-season N recommendation. In the case study, using local soil sampling data for mode calibration was not tested, because it is inefficient and not scalable. Abundant continuous soil moisture observations at different soil depth are available from stations affiliated with various networks (e.g. AmeriFlux, llinois, USA Climate Network and ISU Soil Moisture Network). However, their limited spatial distribution, along with considerable soil heterogeneity, make them unsuitable for directly comparing model simulated soil moisture for a particular site to any measurements from a neighboring station (not to mention the nearest station is usually miles away). One possible way to use these measurements is to do calibration at individual sites and then extrapolate the optimized parameters based on their relationships with more easily accessible information such as soil texture. However, the numerical uncertainty introduced in the calibration procedures may jeopardize this method, making it no better than using empirical relationships provided in the literature. For example, Saxton et al. (1986) introduced a method (Saxton method hereafter) to estimate generalized soil hydraulic characteristics from soil texture, and released an updated version with additional field measurements (Saxton and Rawls 2006). When comparing soil hydraulic parameters calculated by the Saxton method to values obtained from SSURGO, the two sets had similar values. In addition, as is discussed in the previous section, these parameters can be estimated based on aboveground information using inverse modeling techniques (Charoenhirunyingyos et al. 2011). Determining SOC is even more challenging, because the traditional soil sampling is labor and cost intensive and suffers from a high spatial uncertainty (Scharf 2015). Simple, reliable and scalable methods to estimate the spatial heterogeneity in SOC are still lacking. Soil reflectance (color) has the potential to fill this gap, but results obtained using this method so far can be only treated as preliminary (Gomez et al. 2008; Ladoni et al. 2010). In addition, some recent studies show the potential to fine tune SSURGO data based on layers of information such as topography (Ashtekar and Owens 2013; Chaney et al. 2016) and hyperspectral imagery.

Conclusions

This study presented a sub-field scale prescription tool for variable rate N fertilization for the US Corn system. The proposed tool employed the crop model simulations to track a range of soil N processes, and used satellite images to derive management zones, to train the crop model and to assess the crop growth status. In a case study, the tool successfully captured the sub-field variability of crop systems. The recommended sidedress N rates enhanced zones with high yield potential, while preventing over-fertilization in zones with

low yield potential. Marginal benefits from sidedress decreased with the increase of fertilizer amount. Model sensitivity analysis indicated that soil hydraulic properties and soil organic carbon content are critical to the reliability of this sidedress N recommendation tool. Crop N uptake at the time of sidedress can be well constrained by calibrating the phenology module using normalized satellite-derived LAI. Compared with other N recommendation tools, the framework presented here is efficient, accurate and scalable and requires less upfront information from users.

Although the prototype introduced in this study can be easily adapted to other crops or regions outside the US, two caveats should be noted. First, information on soil properties is the major source of uncertainty. When abundant aerial images are available (either through satellite or UAV), estimating a few soil parameters using inverse modeling approaches is worth considering. Alternatively, it is desirable to better extrapolate or fine tune existing soil survey data based on layers of information such as ECa, topography and aerial imagery. Second, the performance of the proposed tool is highly relevant to the number of RapidEye images that can be acquired within a growing season. Higher frequency of image collection is highly recommended to further improve this tool. This can be achieved by requesting smaller revisit time from the RapidEye system, by switching to other imagery sources such as the PlanetScope Satellite Constellation, or by using the more manageable UAV monitoring.

References

Abendroth, L. J. (2011). *Corn growth and development*. Ames, IA: Iowa State University Extension.

Archontoulis, S. V., Miguez, F. E., & Moore, K. J. (2014). Evaluating APSIM maize, soil water, soil nitrogen, manure, and soil temperature modules in the Midwestern United States. *Agronomy Journal, 106,* 1025–1040.

Arthur, D., & Vassilvitskii, S. (2007). k-means++: The advantages of careful seeding. In *Proceedings of the eighteenth annual ACM-SIAM symposium on Discrete algorithms* (pp. 1027–1035). New Orleans, LS, USA: Society for Industrial and Applied Mathematics.

Ashtekar, J. M., & Owens, P. R. (2013). Remembering knowledge: An expert knowledge based approach to digital soil mapping. *Soil Horizons, 54,* 1–6.

Cassman, K. G., Dobermann, A., & Walters, D. T. (2002). Agroecosystems, nitrogen-use efficiency, and nitrogen management. *AMBIO: A Journal of the Human Environment, 31,* 132–140.

Castaldi, F., Palombo, A., Santini, F., Pascucci, S., Pignatti, S., & Casa, R. (2016). Evaluation of the potential of the current and forthcoming multispectral and hyperspectral imagers to estimate soil texture and organic carbon. *Remote Sensing of Environment, 179,* 54–65.

Chander, G., Haque, M. O., Sampath, A., Brunn, A., Trosset, G., Hoffmann, D., et al. (2013). Radiometric and geometric assessment of data from the RapidEye constellation of satellites. *International Journal of Remote Sensing, 34,* 5905–5925.

Chaney, N. W., Wood, E. F., McBratney, A. B., Hempel, J. W., Nauman, T. W., Brungard, C. W., et al. (2016). POLARIS: A 30-meter probabilistic soil series map of the contiguous United States. *Geoderma, 274,* 54–67.

Charoenhirunyingyos, S., Honda, K., Kamthonkiat, D., & Ines, A. V. (2011). Soil moisture estimation from inverse modeling using multiple criteria functions. *Computers and Electronics in Agriculture, 75,* 278–287.

Cicore, P., Serrano, J., Shahidian, S., Sousa, A., Costa, J. L., & da Silva, J. R. M. (2016). Assessment of the spatial variability in tall wheatgrass forage using LANDSAT 8 satellite imagery to delineate potential management zones. *Environmental Monitoring and Assessment, 188,* 513.

Derby, N. E., Casey, F. X. M., & Franzen, D. W. (2007). Comparison of nitrogen management zone delineation methods for corn grain yield. *Agronomy Journal, 99,* 405–414.

Diker, K., Heermann, D. F., & Brodahl, M. K. (2004). Frequency analysis of yield for delineating yield response zones. *Precision Agriculture, 5,* 435–444.

Fleming, K. L., Heermann, D. F., & Westfall, D. G. (2004). Evaluating soil color with farmer input and apparent soil electrical conductivity for management zone delineation. *Agronomy Journal, 96,* 1581–1587.

Gitelson, A. A. (2004). Wide dynamic range vegetation index for remote quantification of biophysical characteristics of vegetation. *Journal of Plant Physiology, 161,* 165–173.

Gomez, C., Viscarra Rossel, R. A., & McBratney, A. B. (2008). Soil organic carbon prediction by hyper-spectral remote sensing and field vis-NIR spectroscopy: An Australian case study. *Geoderma, 146,* 403–411.

Guastaferro, F., Castrignanò, A., De Benedetto, D., Sollitto, D., Troccoli, A., & Cafarelli, B. (2010). A comparison of different algorithms for the delineation of management zones. *Precision Agriculture, 11,* 600–620.

Hammer, G. L., Dong, Z., McLean, G., Doherty, A., Messina, C., Schussler, J., et al. (2009). Can Changes in canopy and/or root system architecture explain historical maize yield trends in the U.S. Corn Belt? *Crop Science, 49,* 299–312.

Hank, T. B., Bach, H., & Mauser, W. (2015). Using a remote sensing-supported hydro-agroecological model for field-scale simulation of heterogeneous crop growth and yield: Application for wheat in central Europe. *Remote Sensing, 7,* 3934–3965.

Holzworth, D. P., Huth, N. I., deVoil, P. G., et al. (2014). APSIM—evolution towards a new generation of agricultural systems simulation. *Environmental Modelling and Software, 62,* 327–350.

Honda, K., Ines, A. V., Yui, A., Witayangkurn, A., Chinnachodteeranun, R., & Teeravech, K. (2014). Agriculture information service built on geospatial data infrastructure and crop modeling. In *Proceedings of the 2014 international workshop on web intelligence and smart sensing* (pp. 1–9). New York, USA: Association for Computing Machinery.

Hunt, E. R., Hively, W. D., Daughtry, C. S., McCarty, G. W., Fujikawa, S. J., Ng, T. L., et al. (2008). Remote sensing of crop leaf area index using unmanned airborne vehicles. In *Proceedings of the Pecora 17 symposium.* Bethesda, MD: American Society for Photogrammetry and Remote Sensing. CDROM. http://www.asprs.org/a/publications/proceedings/pecora17/0018.pdf. Accessed 31 Oct 2016.

Irish, R. R. (2000). Landsat 7 automatic cloud cover assessment. In *AeroSense 2000* (pp. 348–355). Bellingham, WA, USA: International Society for Optics and Photonics.

Jin, Z., Zhuang, Q., He, J.-S., Zhu, X., & Song, W. (2015). Net exchanges of methane and carbon dioxide on the Qinghai-Tibetan Plateau from 1979 to 2100. *Environmental Research Letters, 10,* 085007.

Jin, Z., Zhuang, Q., Tan, Z., Dukes, J. S., Zheng, B., & Melillo, J. M. (2016). Do maize models capture the impacts of heat and drought stresses on yield? Using algorithm ensembles to identify successful approaches. *Global Change Biology, 22,* 3112–3126.

Keeney, D., & Olson, R. A. (1986). Sources of nitrate to ground water. *Critical Reviews in Environmental Control, 16,* 257–304.

Kravchenko, A. N., & Bullock, D. G. (2000). Correlation of corn and soybean grain yield with topography and soil properties. *Agronomy Journal, 92,* 75–83.

Ladoni, M., Bahrami, H., Alavipanah, S., & Norouzi, A. (2010). Estimating soil organic carbon from soil reflectance: A review. *Precision Agriculture, 11,* 82–99.

Littleboy, M., Silburn, D. M., Freebairn, D. M., Woodruff, D. R., Hammer, G. L., & Leslie, J. K. (1992). Impact of soil erosion on production in cropping systems. I. Development and validation of a simulation model. *Soil Research, 30,* 757–774.

Lobell, D. B., Hammer, G. L., McLean, G., Messina, C., Roberts, M. J., & Schlenker, W. (2013). The critical role of extreme heat for maize production in the United States. *Nature Climate Change, 3,* 497–501.

Lobell, D. B., Thau, D., Seifert, C., Engle, E., & Little, B. (2015). A scalable satellite-based crop yield mapper. *Remote Sensing of Environment, 164,* 324–333.

Ma, B. L., & Biswas, D. K. (2015). Precision nitrogen management for sustainable corn production. In *Sustainable agriculture reviews* (pp. 33–62). Cham, Switzerland: Springer International Publishing.

Machwitz, M., Giustarini, L., Bossung, C., Frantz, D., Schlerf, M., Lilienthal, H., et al. (2014). Enhanced biomass prediction by assimilating satellite data into a crop growth model. *Environmental Modelling and Software, 62,* 437–453.

Mamo, M., Malzer, G. L., Mulla, D. J., Huggins, D. R., & Strock, J. (2003). Spatial and temporal variation in economically optimum nitrogen rate for corn. *Agronomy Journal, 95,* 958–964.

McIsaac, G. F., David, M. B., Gertner, G. Z., & Goolsby, D. A. (2002). Relating net nitrogen input in the Mississippi River Basin to nitrate flux in the lower Mississippi River. *Journal of Environmental Quality, 31,* 1610–1622.

Melkonian, J. J., van Es, H. M., DeGaetano, A. T., & Joseph, T. (2008) ADAPT-N: Adaptive nitrogen management for maize using high resolution climate data and model simulations. In: R. Khosla (Ed.), *Proceedings of the 9th international conference on precision agriculture.* Denver, CO. 18–21 July 2010. Monticello, IL, USA: International Society of Precision Agriculture. CDROM.

Moebius-Clune, B., Van Es, H., & Melkonian, J. (2013). Adapt-N uses models and weather data to improve nitrogen management for corn. *Better Crops, 97,* 7–9.

Mulder, V. L., De Bruin, S., Schaepman, M. E., & Mayr, T. R. (2011). The use of remote sensing in soil and terrain mapping—a review. *Geoderma, 162,* 1–19.

Mulla, D. J. (2013). Twenty five years of remote sensing in precision agriculture: Key advances and remaining knowledge gaps. *Biosystems Engineering, 114,* 358–371.

Pappas, C., Fatichi, S., Leuzinger, S., Wolf, A., & Burlando, P. (2013). Sensitivity analysis of a process-based ecosystem model: Pinpointing parameterization and structural issues. *Journal of Geophysical Research: Biogeosciences, 118,* 505–528.

Park, S., Croteau, P., Boering, K. A., Etheridge, D. M., Ferretti, D., Fraser, P. J., et al. (2012). Trends and seasonal cycles in the isotopic composition of nitrous oxide since 1940. *Nature Geoscience, 5,* 261–265.

Prasad, R., Hochmuth, G. J., & Boote, K. J. (2015). Estimation of nitrogen pools in irrigated potato production on sandy soil using the model SUBSTOR. *PLoS ONE, 10,* e0117891.

Randall, G. W., Vetsch, J. A., & Huffman, J. R. (2003). Nitrate losses in subsurface drainage from a corn-soybean rotation as affected by time of nitrogen application and use of nitrapyrin. *Journal of Environmental Quality, 32,* 1764–1772.

Sakamoto, T., Gitelson, A. A., & Arkebauer, T. J. (2014). Near real-time prediction of US corn yields based on time-series MODIS data. *Remote Sensing of Environment, 147,* 219–231.

Saxton, K. E., & Rawls, W. J. (2006). Soil water characteristic estimates by texture and organic matter for hydrologic solutions. *Soil Science Society of America Journal, 70,* 1569–1578.

Saxton, K. E., Rawls, W. J., Romberger, J. S., & Papendick, R. I. (1986). Estimating generalized soil-water characteristics from texture. *Soil Science Society of America Journal, 50,* 1031–1036.

Scharf, P. C. (2015) Managing nitrogen. In: *Managing nitrogen in crop production* (pp. 25–76). Madison, WI, USA: American Society of Agronomy, Inc., Crop Science Society of America, Inc., and Soil Science Society of America, Inc.

Sela, S., van Es, H. M., Moebius-Clune, B. N., Marjerison, R., Melkonian, J., Moebius-Clune, D., et al. (2016). Adapt-N outperforms grower-selected nitrogen rates in Northeast and Midwestern United States strip trials. *Agronomy Journal, 103*(108), 1726–1734.

Setiyono, T. D., Yang, H., Walters, D. T., Dobermann, A., Ferguson, R. B., Roberts, D. F., et al. (2011). Maize-N: A Decision tool for nitrogen management in maize. *Agronomy Journal, 103,* 1276–1283.

Shaddad, S. M., Madrau, S., Castrignanò, A., & Mouazen, A. M. (2016). Data fusion techniques for delineation of site-specific management zones in a field in UK. *Precision Agriculture, 17,* 200–217.

Shahandeh, H., Wright, A. L., & Hons, F. M. (2011). Use of soil nitrogen parameters and texture for spatially-variable nitrogen fertilization. *Precision Agriculture, 12,* 146–163.

Sibley, A. M., Grassini, P., Thomas, N. E., Cassman, K. G., & Lobell, D. B. (2014). Testing remote sensing approaches for assessing yield variability among maize fields. *Agronomy Journal, 106,* 24–32.

Sinclair, T. R., & Muchow, R. C. (1995). Effect of nitrogen supply on maize yield: I. Modeling physiological responses. *Agronomy Journal, 87,* 632–641.

Soil Survey Staff, Natural Resources Conservation Service, United States Department of Agriculture. Web Soil Survey. Retrieved Octobor 31, 2016 from http://websoilsurvey.nrcs.usda.gov/.

Solie, J. B., Monroe, A. D., Raun, W. R., & Stone, M. L. (2012). Generalized algorithm for variable-rate nitrogen application in cereal grains. *Agronomy Journal, 104,* 378–387.

Song, X., Wang, J., Huang, W., Liu, L., Yan, G., & Pu, R. (2009). The delineation of agricultural management zones with high resolution remotely sensed data. *Precision Agriculture, 10,* 471–487.

Thompson, L. J., Ferguson, R. B., Kitchen, N., Frazen, D. W., Mamo, M., Yang, H., et al. (2015). Model and sensor-based recommendation approaches for in-season nitrogen management in corn. *Agronomy Journal, 107,* 2020–2030.

Tibshirani, R., Walther, G., & Hastie, T. (2001). Estimating the number of clusters in a data set via the gap statistic. *Journal of the Royal Statistical Society: Series B (Statistical Methodology), 63,* 411–423.

Tremblay, N., Bouroubi, Y. M., Bélec, C., Mullen, R. W., Kitchen, N. R., Thomason, W. E., et al. (2012). Corn response to nitrogen is influenced by soil texture and weather. *Agronomy Journal, 104,* 1658–1671.

Viña, A., Gitelson, A. A., Nguy-Robertson, A. L., & Peng, Y. (2011). Comparison of different vegetation indices for the remote assessment of green leaf area index of crops. *Remote Sensing of Environment, 115,* 3468–3478.

Wilson, D. R., Muchow, R. C., & Murgatroyd, C. J. (1995). Model analysis of temperature and solar radiation limitations to maize potential productivity in a cool climate. *Field crops research, 43,* 1–18.

Yang, H., Dobermann, A., Cassman, K. G., & Walters, D. T. (2006). Features, applications, and limitations of the Hybrid-Maize simulation model. *Agronomy Journal, 98,* 737–748.

Zhang, X., Shi, L., Jia, X., Seielstad, G., & Helgason, C. (2010). Zone mapping application for precision-farming: A decision support tool for variable rate application. *Precision Agriculture, 11,* 103–114.